

# Chapter 6. Beam Loss, Collimation and Shielding

A.I. Drozhdin, M.A. Kostin, N.V. Mokhov

## 6.1. Beam Loss and Shielding Design Strategy

A high beam power of 0.48 MW implies serious constraints on beam losses in the Proton Driver. As in the previous study [1], the design strategy is that the beam losses are localized and controlled as much as possible via the dedicated beam collimation system. This way, the source term for the radiation analysis is a derivative of the collimation system performance. A high loss rate is localized in the collimation section with components locally shielded to equalize prompt and residual radiation levels in the tunnel and drastically lower uncontrolled beam loss rates in the rest of the lattice [2, 3]. The radiation transport analysis is fundamentally important because of the impact on machine performance, conventional facility design, maintenance operations, and related costs. Results of this chapter are based on detailed Monte Carlo simulations with the STRUCT [4] and MARS [5] codes.

### 6.1.1. Regulatory requirements

1. *Prompt radiation:* the criterion for dose rate in non-controlled areas on accessible outside surfaces of the shield is 0.05 mrem/hr at normal operation and 1 mrem/hr for the worst case due to accidents [6]. Currently, the Fermilab Radiological Control Manual (FRCM) [6] requires that the machine designers describe and justify what a possible “credible worst case accident” is, and design the shielding—or modify operation of the machine—accordingly.

2. *Hands-on maintenance:* anywhere in the machine, residual dose rate  $P_\gamma \leq 100$  mrem/hr = 1 mSv/hr at 30 cm from the component surface, after 100 day irradiation at 4 hrs after shutdown. Averaged over all the components,  $P_\gamma \leq 10 - 20$  mrem/hr = 0.1 - 0.2 mSv/hr.

3. *Ground-water activation:* do not exceed radionuclide concentration limits  $C_{i,reg}$  of 20 pCi/ml for  $^3\text{H}$  and 0.4 pCi/ml for  $^{22}\text{Na}$  in any nearby drinking water supplies. The sum  $C_{tot}$  of the fractions of radionuclide contamination (relative to regulatory limits  $C_{i,reg}$ ) must be less than one for all radionuclides. Corresponding star density and hadron flux are strongly site and depth specific.

Additionally, one assumes the accumulated dose of 20 Mrad/yr or 400 Mrad over 20 years lifetime in the hot spots of machine components as a *radiation damage* limit for such materials as epoxy and cable insulation.

### 6.1.2. Normal operation and beam accident

The radiation analysis for the beam transport lines, arcs and long straight sections is performed both for normal operation and for accidental beam loss. The maximum shielding thickness from the both cases is put into the design as the tunnel shielding in that part of the machine.

In normal operation, the source term is based on the beam loss distributions calculated with a beam collimation system described in the next section. This system provides average rates in the arcs outside the collimation region of about 0.12 W/m at the top energy and less than 0.05 W/m at injection, although some peaks at the top energy are as high as several Watts per meter. This is to be compared to the tolerable beam loss rates for hands-on maintenance of about 0.25 W/m (bare beam pipes) and 3 - 10 W/m (magnets) for  $P_\gamma = 100$  mrem/hr at local peaks and five times lower (0.05 and 0.6 - 2 W/m, respectively) for  $P_\gamma = 20$  mrem/hr averaged over the lattice [1, 2]. At such rates, the peak accumulated dose in the coils is not a limiting factor. For ground-water activation a limiting rate is in the range of about 0.5 to 10 W/m depending on siting.

For accidental beam loss, a *credible* accident is considered: a point-like loss of 0.1% of the full beam intensity during one hour. This is about  $10^{15}$  protons. Once such an accident happens, the machine is shut down within 1 second to analyze the cause and undertake appropriate measures.

## 6.2. Collimation System

### 6.2.1. Beam loss localization

With an assumed 1% (4.8 kW) of the beam lost at the top energy, the peaks (at some quadrupoles) in the beam loss distribution reach several kW/m, a few thousand times higher than the tolerable levels. Therefore, a three-stage beam collimation system is implemented into the lattice. Both of the two 75.4-m long straight sections are occupied by the RF cavities, injection and extraction systems. Due to space constraints, the collimation system is placed in the available drift spaces of the arc section in the slots upstream and downstream of the short dipoles. The system consists of horizontal and vertical primary collimators, four secondary collimators, and two supplementary ones as shown in Fig. 6.1 and Table 6.1.

Secondary collimators need to be placed at phase advances which are optimal to intercept most of particles out-scattered from the primary collimators during the first turn after the halo interaction with the primary collimator. Transverse phase space at the collimators is shown in Fig. 6.2. The optimal phase advances are around  $k \cdot \pi \pm 30^\circ$ . Phase advances between the primary and secondary collimators are presented in Table 6.1. The horizontal

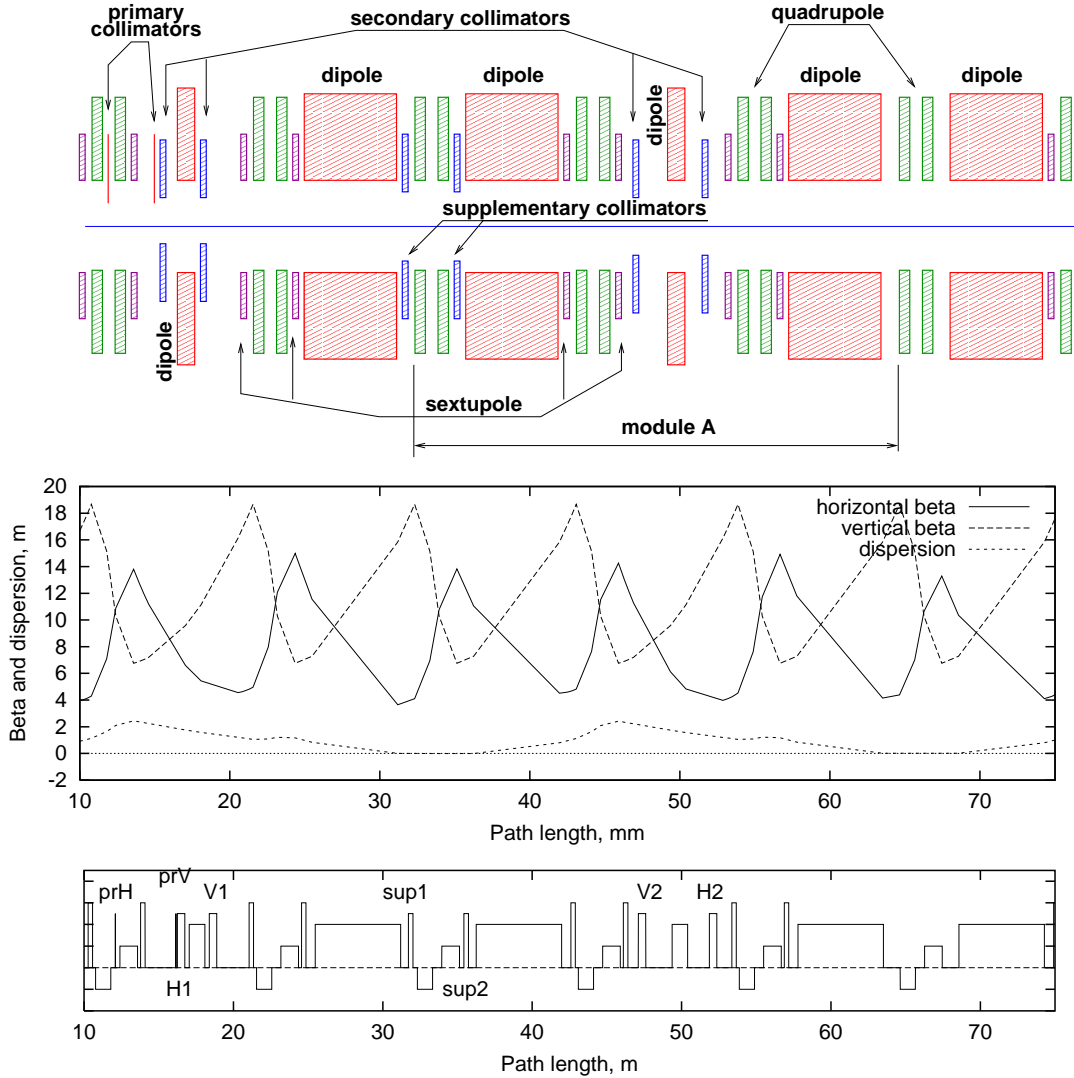


**Figure 6.1.** Beam collimation system (top) and beta functions and dispersion in the collimation section (bottom).

**Table 6.1.**  $\beta$ -functions, dispersion and phase advance between primary and secondary collimators.

Collimator	$\beta$ -function (m)		Dispersion (m)	Phase advance between primary and secondary collimators (deg)	
	horizontal	vertical		horizontal	vertical
Horizontal primary	8.9	12.6	1.9	0	-
Vertical primary	8.0	8.5	1.9	-	0
Secondary H1	7.8	9.2	1.9	24	-
Secondary V1	5.2	12.6	1.5	-	14
Supplementary 1	3.9	17.9	0.0	176	84
Supplementary 2	12.2	7.0	0.0	203	105
Secondary V2	10.7	7.7	2.1	-	172
Secondary H2	4.0	15.0	1.4	348	-

and vertical primary collimators are placed at the edge of the beam after painting, with secondary collimators father from this position by an offset  $d$ . Beam loss distributions at injection and top energies are shown in Fig. 6.3 for the system with 0.3-mm thick tungsten primary collimators, four secondary collimators (0.5-m long stainless steel or copper) positioned at  $d = 2$  mm and two 0.3-m long supplementary collimators at  $d = 4$  mm. It is assumed in calculations that 10% of the beam is lost at injection and 1% at the top energy, and  $2/3$  of these amounts interact the horizontal primary collimator (a half for off-momentum protons with  $\Delta p/p = \pm 0.002$  and a half for on-momentum protons) and  $1/3$  the vertical primary collimator. The  $\beta$ -function varies along the length of a secondary collimator, therefore the collimator apertures are assumed to be tapered to follow the beam envelope after painting.

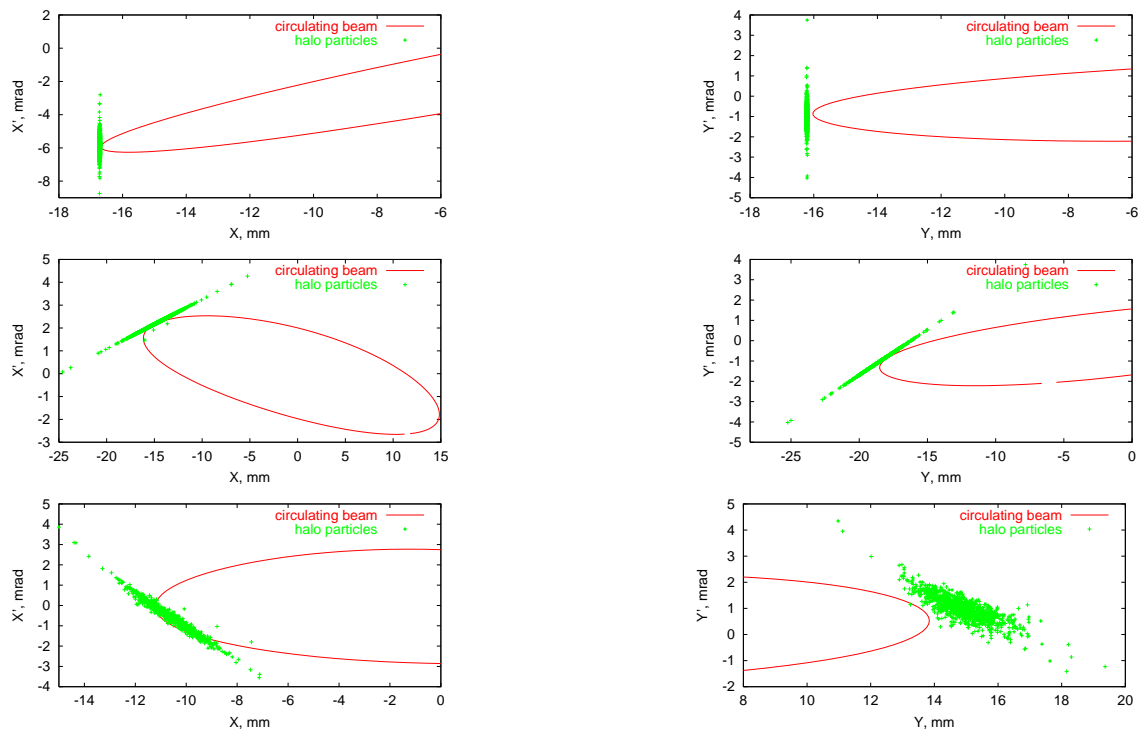


**Figure 6.2.** Horizontal (left) and vertical (right) phase space at the primary collimators (top), secondary collimators 1H and 1V (middle), and collimators 2H and 2V (bottom).

The right side of Fig. 6.3 shows details of beam loss in the collimation region. Secondary collimators generate out-scattered particles lost later in the lattice. One can reduce this component with a *3-stage collimation system*. Several *main* secondary collimators are positioned close to the beam to deal with protons scattered in the primary collimator and several *supplementary* collimators are farther from the beam to catch particles out-scattered from the main secondary collimators. A significant reduction of beam loss rates by introducing 2 supplementary collimators 0.3-m long positioned at  $d = 4$  mm is seen by comparing the middle and bottom plots in Fig. 6.3. Total beam losses in the collimation section and in the rest of the machine along with the peak loss rates are presented in

Table 6.2 for both top and injection energies. Results are given for the machine without collimators and for the collimation system with primary collimators of various thicknesses  $t$ , secondary collimators at  $d = 2$  mm and with and without two supplementary collimators at offset of  $d = 4$  mm with respect to the primary collimators.

With the proposed system,  $\sim 99\%$  of the beam halo energy is intercepted in the 58-m long arc section. About 1% is lost in the rest of the machine along 416-m length with mean rate of 0.12 W/m. At several locations the beam loss is noticeably higher, exceeding the tolerable rates. Such “hot” locations need special care. Beam loss rates in the collimation system section itself are very high requiring a special shielding design (see next section).

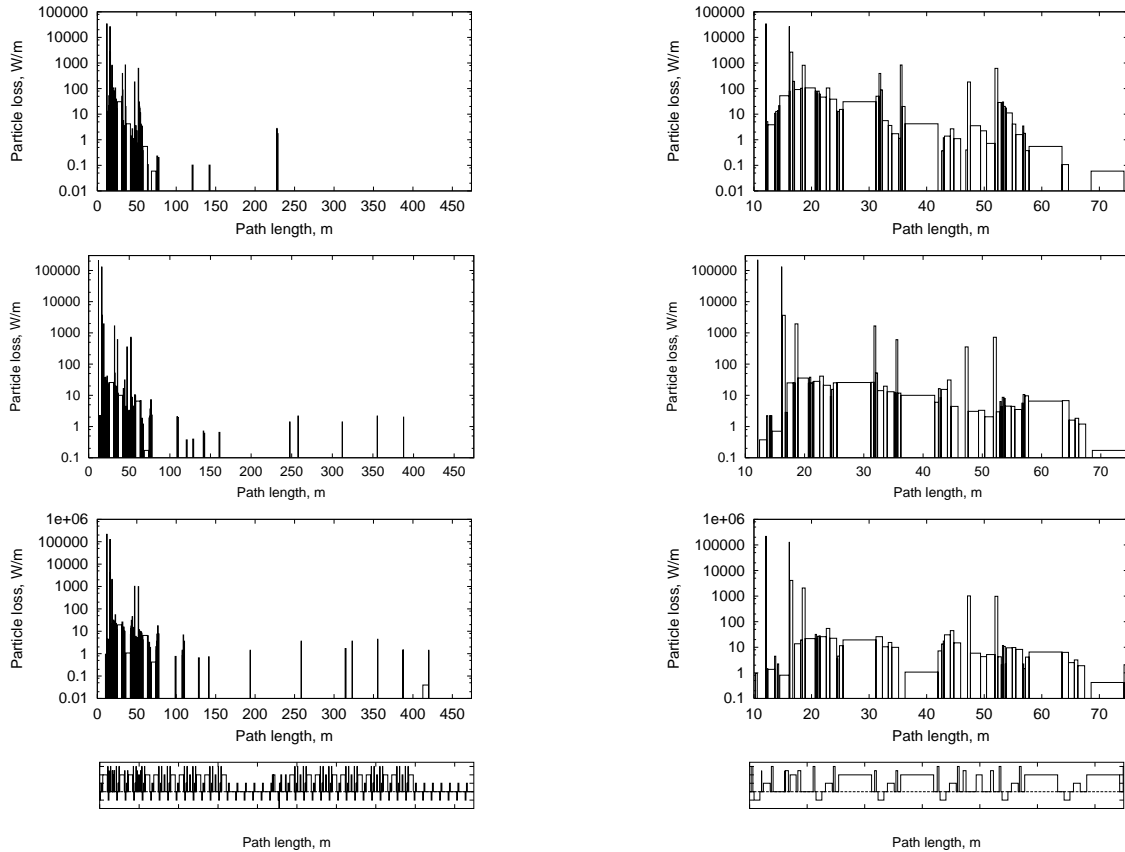


**Figure 6.3.** Beam loss distributions at injection (top) and at top energy with (middle) and without (bottom) supplementary collimators. The left group shows the entire machine and the right group shows the collimation region.

### 6.2.2. Mechanical design

The mechanical design of the secondary collimators is similar to that of those already built and installed in the Tevatron for Collider Run II [7]. The collimator jaws consist of two pieces 30-40 mm wide welded together in an 130-mm “L” configuration. Primary

**Table 6.2.** Total beam losses in the 58-m collimation section ( $P_{coll}$ ) and in the rest of the lattice ( $P_{rest}$ ) and peak beam loss rates in the rest of the machine ( $p_{peak}$ ).

Primary collimator thickness	$P_{coll}$ (kW)	$P_{rest}$ (kW)	$p_{peak}$ (W/m)
$E_{kin} = 8$ GeV without collimation			
	0.310	4.489	5900
$E_{kin} = 8$ GeV without supplementary collimators			
$t = 0.1$ mm	4.768	0.035	8
$t = 0.3$ mm	4.753	0.048	7
$t = 0.5$ mm	4.749	0.051	9
$t = 1.0$ mm	4.742	0.058	7
$t = 1.5$ mm	4.743	0.057	8
$E_{kin} = 8$ GeV with supplementary collimators			
$t = 0.3$ mm	4.778	0.024	2
$E_{kin} = 0.6$ GeV with supplementary collimators			
$t = 0.3$ mm	3.596	0.005	0.2

collimators are made of tungsten 1 mm thick. Secondary and supplementary collimators are made of stainless steel or copper (choice will be the subject of further thermal analyses) 0.5 m (secondary) and 0.3 m (supplementary) long. These dimensions will accommodate the full beam size, after painting, as well as maximum impact parameters. Machining and assembly tolerances of  $25 \mu\text{m}$  are easily met for the collimator jaws. All collimators will be in a fixed position during the machine cycle, but motion control is required in order to adjust collimators to their optimum position. The collimator assembly is welded inside a stainless steel box with bellows on each end (Fig. 6.4).

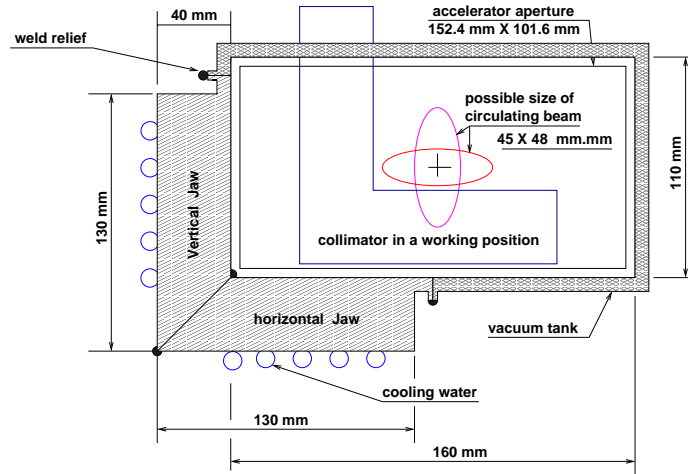


**Figure 6.4.** Collimator cross section.

The box assembly is supported by a cradle which is moved independently in the vertical and horizontal directions by stepping motors. Full range of motion is 50 mm in steps as small as  $25 \mu\text{m}$  if required and a maximum speed of 2.5 mm/sec. The collimator speed can be increased if a larger minimum step size is acceptable. Position readback is provided by linear differential voltage transformers, although investigation into the radiation hardness

of these devices is required. Mechanical damage is prevented by limit switches on all degrees of motion. The entire assembly, including bellows, will occupy approximately 1 m of lattice space.

The primary collimator assembly is identical to the secondary collimator assembly except that their “L” blocks are only 0.1 m in length. The 1-mm thick machined tungsten jaws are bolted to the stainless steel blocks. The blocks provide a good heat sink for energy dissipated in the tungsten. The entire assembly, including bellows, will occupy approximately 0.6 m of lattice space.

The motion controls for the collimators will be similar to the Tevatron system [7]. Up to 4 motors and 4 position readbacks will be controlled and monitored by a single MVME162 processor running VXWORKS in a VME crate in a nearby service building. Stepping motors and LVDT’s are interfaced to the CPU via commercial IP’s (Industrial Packs). The motor PS and motor controllers are also commercial hardware. A total of 3 “stations” – VME crate, motor controller crate, and motor PS will be required for the entire system of 10 collimators. A total of 8.4 kW of DC power (3.6 kW at injection and 4.8 kW at top energy) is expected to be dissipated in all the collimators. This power can be removed from each collimator by circulating LCW (Low Conductivity Water) through cooling channels on the outside of the collimator box. A flow of 1.6 gpm will remove the power with a temperature rise of 20°C. Good thermal contact between the stainless steel “L” blocks and the welded box is required.

## **6.3. Radiation Analysis**

### **6.3.1. Collimation region**

MARS calculations show that residual dose rates on the collimators and magnets of the 58-m collimation system significantly exceed the hands-on maintenance limits (Fig. 6.5(a)). To reduce these levels and protect ground water outside the tunnel walls, the entire region needs to be shielded. The proposed configuration, based on optimizational MARS calculations, consists of steel shielding uniform in two sections: first, 5-m long, starts 0.5 m upstream of the secondary collimator H1 and second is in the remaining downstream region. The first section is 1 m (vertically) and 1.3 m (horizontally) thick on each side of the secondary collimators and 0.6-m around magnets. The second section is 0.65-m (vertically) and 0.95-m (horizontally) thick on each side of the collimators, 0.25-m around dipoles, and 0.4 m (vertically) and 0.7 m (horizontally) around quadrupoles (Fig. 6.5(b)). This reduces residual dose rates below the limits (Fig. 6.5(a)) and provides adequate protection of cables and other components in the tunnel and ground water around the tunnel (Fig. 6.6(a)).

The shielding proposed equalizes (to some extent) the radiation source term outside the shielding and unshielded components further downstream. This allows for the uniform

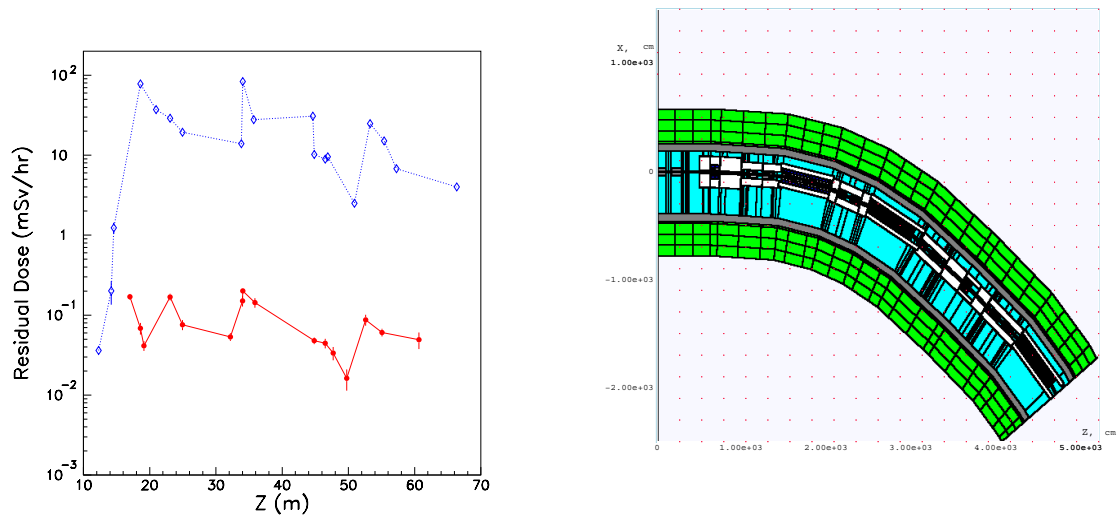


**Figure 6.5.** (a) Maximum contact dose on site surfaces of collimation section components (diamonds) and shielding (circles) (left). (b) MARS model of the 58-m collimation section with steel shielding (right)

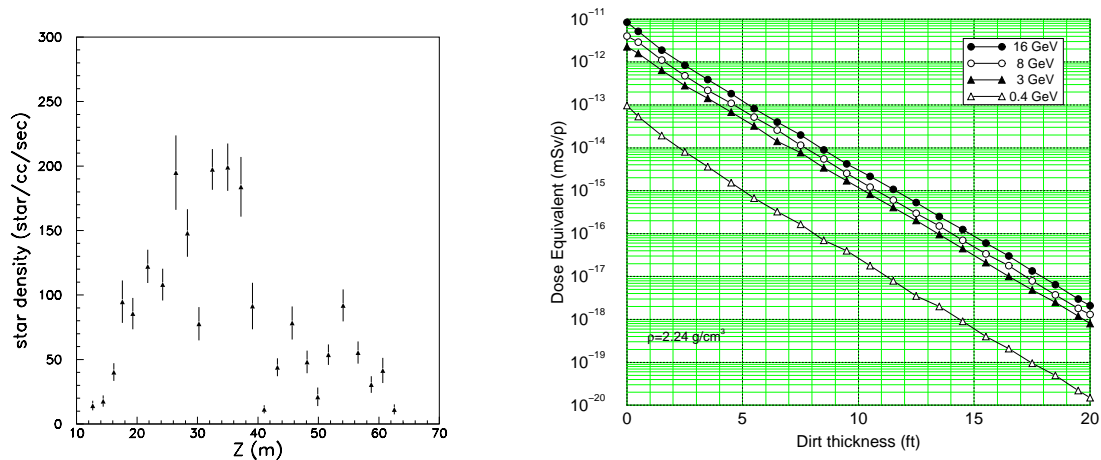


**Figure 6.6.** (a) Radiation load (star density) in the first 20-cm layer of dirt around the collimation section tunnel (left). (b) Prompt dose equivalent vs dirt thickness around the tunnel at a point-like proton loss at four energies (right)

approach to the dirt shielding calculation in the entire machine. The dose on the outer shielding surface depends on the beam energy in a complex way. Assuming a quasi-local beam loss in the magnet, the dose equivalent was calculated with MARS14 as a function of Fermilab wet dirt thickness ( $\rho = 2.24 \text{ g/cm}^3$ ) outside the tunnel walls. Fig. 6.6(b) shows this dependence for kinetic beam energies from 400 MeV to 16 GeV. The dose at high energies scales as  $E^\alpha$ , where  $\alpha$  is about 0.8, while  $\alpha \geq 1$  at  $E \leq 1 \text{ GeV}$ . In addition, a safety factor of three is applied in calculating a final shielding thickness.



To accommodate the collimation system, the first 58 meters of the arc downstream of the injection straight section have a tunnel 19-foot wide, 12-foot high. Its concrete walls are 27-inch thick. The ceiling and floor are 42-inch thick. Fig. 6.7 shows isoflux and isodose contours in the hottest dipole between the secondary collimators H1 and V1, its 1-m shielding and tunnel cross-section. With the shielding, radiation levels outside the tunnel wall are very close to those in the arcs (see below). Therefore, the same external shielding design both for normal operation and beam accident is applied. With a safety factor of 3, the thickness of dirt shielding above this 58-m long region is 19 feet. The maximum dose accumulated in the collimators and hottest spots of the magnet coils reaches 200 Mrad/yr. The maximum yearly dose at cable locations is about 150 krad per year.

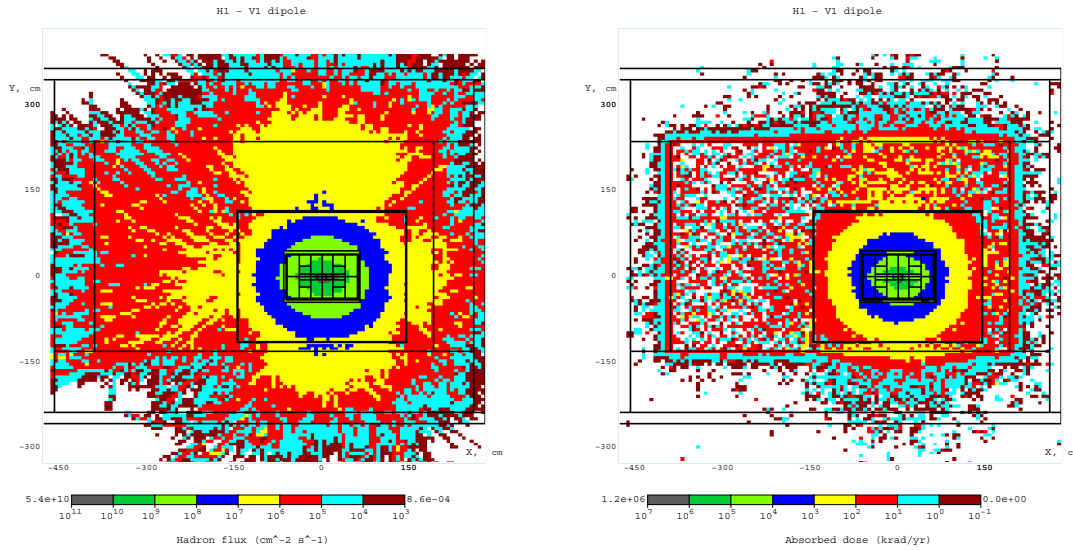


**Figure 6.7.** (a) Hadron ( $E > 20$  MeV) isofluxes ( $\text{cm}^{-2}\text{s}^{-1}$ ) in the tunnel around the dipole between collimators H1 and V1 (left). (b) Yearly isodose contours (krad/yr) at the same location (right).

### 6.3.2. Linac and beam transport lines

In the Linac and injection beam line, assume a proton beam with  $E_{kin} = 600$  MeV at 15 Hz of  $2.8 \times 10^{13}$  protons per pulse,  $4.2 \times 10^{14}$  protons per second with beam power of 40 kW. For a credible accident, the dose immediately outside the tunnel concrete walls is  $6.3 \times 10^3$  mrem/hr. This requires 11 feet of dirt to reduce the dose to 1 mrem/hr, or 12.5 feet with a safety factor of 3. In normal operation with a beam loss rate of 0.16 W/m, the required shield thickness is one foot less. At extraction, an accidental 8-GeV beam loss of  $3.75 \times 10^{14}$  (p/sec) requires 16 feet of dirt. An operational 8-GeV beam loss of  $3.75 \times 10^8$  (p/m/sec) = 0.48 W/m along a 1000-m long extraction beam line requires 13.5 feet of dirt. Assuming a safety factor of 3, the thickness of dirt shielding above the 8-GeV extraction beam line is 17.5 feet.

### 6.3.3. Long straight sections

Two long straight sections accommodate injection, extraction and RF systems. The tunnel width is 19 feet, its height is 12 feet, the concrete walls are 15-inch thick, ceiling and floor are 30-inch thick. Extraction will be one-turn fast extraction with very little loss at the extraction septum as in Ref. [1]. When the machine is well tuned, the extraction loss can be as low as the order of  $10^{-4}$ , which has been achieved at the ISIS. As for the RF cavities with large apertures, our calculations show no noticeable beam loss in those regions. This implies that no local shielding is needed in the long straight sections. At this stage, shielding design and radiation requirements in these regions are assumed the same as in the arcs.

### 6.3.4. Arcs

The full arc lattice in a rectangular tunnel embedded into wet Fermilab dirt is implemented into the MARS calculation model. The tunnel width is 16 feet, its height is 9 feet, the concrete walls are 15-inch thick, ceiling and floor are 30-inch thick. Cable trays are positioned at the ceiling in the left and right corners of the cross-sections. The arc that follows the injection straight section is enlarged in the first 58 meters to accommodate the collimation system and is considered separately in the next sub-section. Because of non-uniform beam loss in the arcs (see Figs. 6.3) and the absence of self-shielding by magnet bodies, there are always pronounced radiation peaks of field around the long bare beam pipes. At some of these locations, the radiation levels are 2 to 4 times higher than the limits, requiring either further reduction of beam loss rates or a simple thin local shields. Around the magnets—due to absorption of radiation in their material—the flux and, as a result, all other radiation values are several times lower.

Despite the variation in beam loss distribution along the lattice and because the shield thickness is driven by accidental beam loss which can take place in an arbitrary lattice location, a uniform shielding design along the arcs is proposed. With a point-like accidental loss of 0.1% of the 1-hour beam intensity at 8 GeV, the shield thickness required is 17.5 feet of Fermilab wet dirt. During normal operation the earth shielding required to reduce the dose to 0.05 mrem/hr is  $\sim 14$  feet. This is based on the loss rate in the magnets normalized to 1 W/m. Assuming a safety factor of 3, the thickness of dirt shielding above the arcs, driven by accidental loss, is 19 feet.

The maximum dose accumulated in the coils is about 1 Mrad/yr which is acceptable with the use of appropriate materials for insulation. The maximum dose at cable locations is about 0.005 Mrad/yr around the hot spots in the magnets, and is about 0.05 Mrad/yr around long bare beam pipes at the same beam loss rate. At several locations, calculated peak residual dose rates near the bare beam pipes exceed the design goal for hot regions of 100 mrem/hr, being noticeably lower near the magnets due to significant absorption of soft

photons in the dipole and quadrupole materials. The hands-on maintenance criterion gives about 3 W/m for a tolerable maximum beam loss rate in the lattice elements, except for the long bare beam pipes where one should decrease the loss rate to 0.25 W/m to reduce the dose to 100 mrem/hr. One needs further reduction to bring the dose down to a good practice value of about 10-20 mrem/hr. Alternatively, one can think of providing simple shielding around the bare beam pipes. With these measures, the above problem with ground water activation—if it exists at the site—is solved.

## References

- [1] “The Proton Driver Design Study” FERMILAB-TM-2136, December 2000.
- [2] A.I. Drozhdin, O.E. Krivosheev, N.V. Mokhov, “Beam Loss and Collimation in the Fermilab 16-GeV Proton Driver”, Proc. 2001 Particle Accelerator Conference, Chicago, p. 2572 (2001); Fermilab-Conf-01/128 (2001).
- [3] N.V. Mokhov, A.I. Drozhdin, O.E. Krivosheev, “Radiation Shielding of the Fermilab Proton Driver”, Proc. 2001 Particle Accelerator Conference, Chicago, p. 2578 (2001); Fermilab-Conf-01/132 (2001).
- [4] I.S. Baishev, A.I. Drozhdin, N.V. Mokhov, “STRUCT Program User’s Reference Manual”, SSCL-MAN-0034 (1994); <http://www-ap.fnal.gov/~drozhdin/>.
- [5] N. V. Mokhov, “The MARS Code System User’s Guide”, Fermilab-FN-628 (1995); N. V. Mokhov and O. E. Krivosheev, “MARS Code Status”, Fermilab-Conf-00/181 (2000); <http://www-ap.fnal.gov/MARS/>.
- [6] “Fermilab Radiological Control Manual”, Article 236, <http://www-esh.fnal.gov/FRCM/>.
- [7] M. Church, A.I. Drozhdin, A. Legan, N.V. Mokhov, R. Reilly, “Tevatron Run-II Beam Collimation System”, Proc. 1999 Particle Accelerator Conference, New York, p. 56 (1999); Fermilab-Conf-99/059 (1999).